

First Observation of an Acetate Switch in a Methanogenic Autotroph (*Methanococcus maripaludis* S2)

Microbiology Insights
Volume 13: 1–7
© The Author(s) 2020
Article reuse guidelines:
sagepub.com/journals-permissions
DOI: 10.1177/1178636120945300



Chi Hung Vo^{1,2} , Nishu Goyal³, Iftekhar A Karimi^{1,2} and Markus Kraft^{2,4,5} 

¹Department of Chemical and Biomolecular Engineering, National University of Singapore, Singapore. ²Cambridge Centre for Advanced Research and Education in Singapore Ltd, Singapore. ³Department of Chemical Engineering, University of Petroleum and Energy Studies, Dehradun, India. ⁴Department of Chemical Engineering and Biotechnology, University of Cambridge, Cambridge, UK. ⁵School of Chemical and Biomedical Engineering, Nanyang Technological University, Singapore.

ABSTRACT: The transition from acetate production by a microorganism in its early growth phase to acetate re-uptake in its late growth phase has been termed acetate switch. It has been observed in several heterotrophic prokaryotes, but not in an autotroph. Furthermore, all reports hitherto have involved the tricarboxylic acid cycle. This study reports the first observation of acetate switch in a methanogenic autotroph *Methanococcus maripaludis* S2, which uses the Wolfe cycle for its anaerobic respiration. When grown in minimal medium with carbon dioxide as the sole carbon source, and either ammonium or dinitrogen as the sole nitrogen source, *M. maripaludis* S2 dissimilated acetate in the early growth phase and assimilated it back in the late growth phase. The acetate switch was more pronounced in the dinitrogen-grown cultures. We postulate that the acetate dissimilation in *M. maripaludis* S2 may serve as a metabolic outlet for the carbon overflow in the early growth phase, and the assimilation in the late growth phase may be due to the scarcity of the carbon source. Based on the primary and secondary protein structures, we propose that MMP0253 may function as the adenosine diphosphate (ADP)-forming acetyl-CoA synthetase to catalyse acetate formation from acetyl-CoA. To verify this, we produced MMP0253 via the ligation-independent cloning technique in *Escherichia coli* strain Rosetta (DE3) using pNIC28-Bsa4 as the vector. The recombinant protein showed catalytic activity, when added into a mixture of acetyl-CoA, ADP, and inorganic phosphate (P_i). The concentration profile of acetate, together with the enzymatic activity of MMP0253, shows that *M. maripaludis* S2 can produce acetate and exhibit an acetate switch.

KEYWORD: acetate switch, acetate dissimilation, acetate assimilation, *Methanococcus maripaludis*, ADP-forming acetyl-CoA synthetase, Acd

RECEIVED: April 9, 2020. **ACCEPTED:** July 1, 2020.

TYPE: Original Research

FUNDING: The author(s) disclosed receipt of the following financial support for the research, authorship, and/or publication of this article: This research is supported by the National Research Foundation, Prime Minister's Office, Singapore, under its CREATE programme. Concomitantly, this work is supported by the National University of Singapore through its Graduate Research Scholarship. This work also received partial

financial support under a Tier 1 grant R-279-000-541-114 from the Ministry of Education, Singapore.

DECLARATION OF CONFLICTING INTERESTS: The author(s) declared no potential conflicts of interest with respect to the research, authorship, and/or publication of this article.

CORRESPONDING AUTHOR: Iftekhar A Karimi, Department of Chemical and Biomolecular Engineering, National University of Singapore, 4 Engineering Drive 4, Singapore 117585. Email: cheiak@nus.edu.sg

Introduction

Many microorganisms alternate their metabolic pathways to adapt to the nutrients in their immediate environments. They prioritise growth when nutrients are abundant and survival when they are scarce. One such behaviour is the 'acetate switch', which has been studied extensively in *Escherichia coli*.¹ Acetate switch involves the transition from acetate dissimilation (production and secretion) to assimilation (uptake and utilisation). In the early growth phase, *E. coli* dissimilates acetate when the carbon flux into the cells exceeds the capacity of its central pathways or when its tricarboxylic acid (TCA) cycle does not operate fully due to limited oxygen.¹ This dissimilation allows *E. coli* to generate adenosine triphosphate (ATP) and reduce acetyl-CoA (Ac-CoA) accumulation.¹ In the later growth phase, when the metabolic bottleneck allows the uptake of acetate due to respiratory capacity, *E. coli* switches to acetate assimilation. The acetate switch is defined as the point where acetate dissimilation equals assimilation. Figure 1 illustrates a typical acetate switch profile in *E. coli*. Besides *E. coli*, acetate

switch has been observed in several other bacteria^{2–4} and 3 halophilic archaea.⁵ To date, all reported cases have involved heterotrophs and the TCA cycle.

This study reports the first observation of an acetate switch in a methanogenic autotroph, specifically *Methanococcus maripaludis* S2. This archaeon is mesophilic, hydrogenotrophic,⁶ and can thrive on minimal nutrients, carbon dioxide (CO₂) as the sole carbon source, and either ammonium or dinitrogen (N₂) as the sole nitrogen source. Acetate assimilation by adenosine monophosphate (AMP)-forming acetate-CoA ligase (Acs) is a known phenomenon⁷ in *M. maripaludis* S2. However, the only record of acetate dissimilation by *M. maripaludis* S2 is the work of Abdel Azim et al,⁸ who reported an acetate concentration of about 1 mmol/L after incubating *M. maripaludis* for 150 hours in a minimal medium supplemented with propionate. Other methanogens such as *Methanosphaera stadtmanae*,⁹ *Methanococcus voltae*,¹⁰ *Methanospirillum hungatei*,¹¹ and *Methanobrix* sp.¹² are known to assimilate acetate, but have not been reported to produce acetate. On the other hand, *Methanococcus jannaschii*¹³ can



Creative Commons Non Commercial CC BY-NC: This article is distributed under the terms of the Creative Commons Attribution-NonCommercial 4.0 License (<https://creativecommons.org/licenses/by-nc/4.0/>) which permits non-commercial use, reproduction and distribution of the work without further permission provided the original work is attributed as specified on the SAGE and Open Access pages (<https://us.sagepub.com/en-us/nam/open-access-at-sage>).

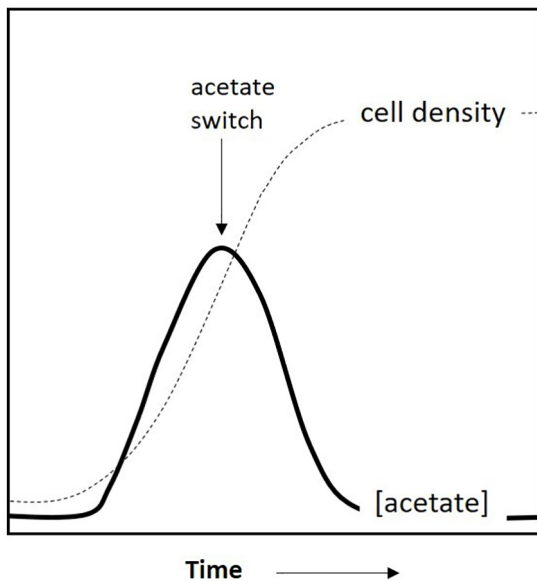


Figure 1. A schematic of acetate switch profile. Acetate concentration increases to a maximum in the early growth phase and decreases thereafter. Acetate concentration reaches zero as the cells enter the stationary phase.

dissimilate acetate, but is unable to assimilate it. Notably, *Methanosarcina acetivorans*¹⁴ and the non-methanogenic *Pyrobaculum islandicum*¹⁵ can both dissimilate and assimilate acetate, but under different growth conditions. No methanogen or autotroph has been reported to display an acetate switch.

In this study, batch culture experiments of *M. maripaludis* S2 were performed in a minimal medium (void of propionate) to investigate its acetate switch. CO₂ and either ammonium or N₂ were used as the sole carbon and nitrogen sources, respectively. As adenosine diphosphate (ADP)-forming Ac-CoA synthetase (Acd) is known¹⁶ to catalyse reversible formation of acetate from Ac-CoA in some other archaea, we propose MMP0253 (GenBank accession no. CAF29809) as the putative Acd in *M. maripaludis*. We produced it and confirmed its enzymatic activity.

Materials and Methods

Gases and chemicals

Pure H₂, CO₂, N₂, and CH₄ gases were purchased from AIR Liquide, Singapore. Mass flow controllers (Red-Y Compact 2 Series, Vögtlin Instruments, Basel-Landschaft, Switzerland) were used to prepare gas mixtures (H₂/CO₂ and H₂/CO₂/N₂). K₂HPO₄, MnSO₄·H₂O, and NH₄Cl were obtained from VWR, Singapore. Nitrilotriacetic acid and Na₂S·9H₂O were purchased from Thermo Fisher Scientific, New Jersey, United States. Other chemicals, if not stated otherwise, were purchased from Sigma-Aldrich, Singapore.

Strain and medium preparation

Methanococcus maripaludis S2 (DSM 14266) was purchased from Leibniz Institute DSMZ-German Collection of Microorganisms and Cell Cultures. Ammonium samples were

prepared as reported.¹⁷ No carbon source was added into the medium and vitamins were also omitted. In N₂ samples, NH₄Cl was omitted in the minimal medium and Fe(NH₄)₂(SO₄)₂·6H₂O was replaced by 140 μL of FeSO₄·7H₂O solution (0.01% w/v). About 460 mL of the minimal medium was dispensed into 1 L serum bottles (Chemglass Life Sciences LLC, New Jersey, USA). To create an anaerobic environment, the bottles were flushed with 80/20 v/v H₂/CO₂ gas mixture at 2 bars for 30 minutes. Subsequently, the bottles were sterilised by autoclaving at 121°C for 21 minutes. After the bottles had cooled down to room temperature, 2.0 mL of Na₂S stock solution (12.5% w/v) was injected into each bottle.

Batch cultivation

The inoculum was pre-cultured for 2 days in the respective minimal medium. At the start of the experiment, 40 mL of the pre-cultured inoculum was transferred to each serum bottle containing fresh medium. H₂/CO₂ gas mixture (74%-85% of H₂ by volume, balance was CO₂) was used to pressurise the ammonium-grown cultures to 259-265 kPa. H₂/CO₂/N₂ gas mixture (68%-73% H₂% and 10%-17% CO₂ by volume, balance was N₂) was used to pressurise the N₂-grown cultures to 304-313 kPa. The cultures were incubated at 37°C and 180 rpm (Orbital Shaking Incubator LM-570RD, Yihder, China). Minimal medium without inoculum was used as a negative control. At the start of each day, the bottles were de-pressurised, flushed, and re-pressurised with H₂/CO₂ and H₂/CO₂/N₂, respectively. At the end of each day, the cultures were kept at 20°C without shaking, until the following morning. All growth experiments were performed in duplicates.

Analytical procedures

About 2 mL of liquid sample was withdrawn hourly using a disposable hypodermic needle (25G × 1", Terumo Corporation, USA) attached to a sterile disposable syringe (3 mL, Nipro Medical Corporation, USA) and deposited in a quartz cell (Agilent Technologies, USA). The optical densities of the samples were measured at 600 nm using a double-beam UV/Vis spectrophotometer (Agilent Technologies, Carry, USA). The concentration of acetate in the liquid sample was determined by a high-performance liquid chromatography (HPLC) (1260 Infinity I, Agilent Technologies, USA) equipped with Aminex HPX-87H column and G7165A multiple wavelength detector (190-240 nm). About 5 mM of H₂SO₄ solution at 0.5 mL/min was used as the mobile phase. The column oven was set at 60°C. The liquid samples were centrifuged at 20 g for 5 minutes before analysis. Acetate was calibrated using standard solutions at 0.01, 0.05, 0.1, 0.25, 0.5, and 0.75 mM. Two additional methods were used to confirm the presence of acetate: gas chromatography (GC) (PerkinElmer Clarus 580, USA) and 500 MHz proton nuclear magnetic resonance (NMR) spectroscopy (Bruker, USA). A control sample with minimal medium and no inoculum was

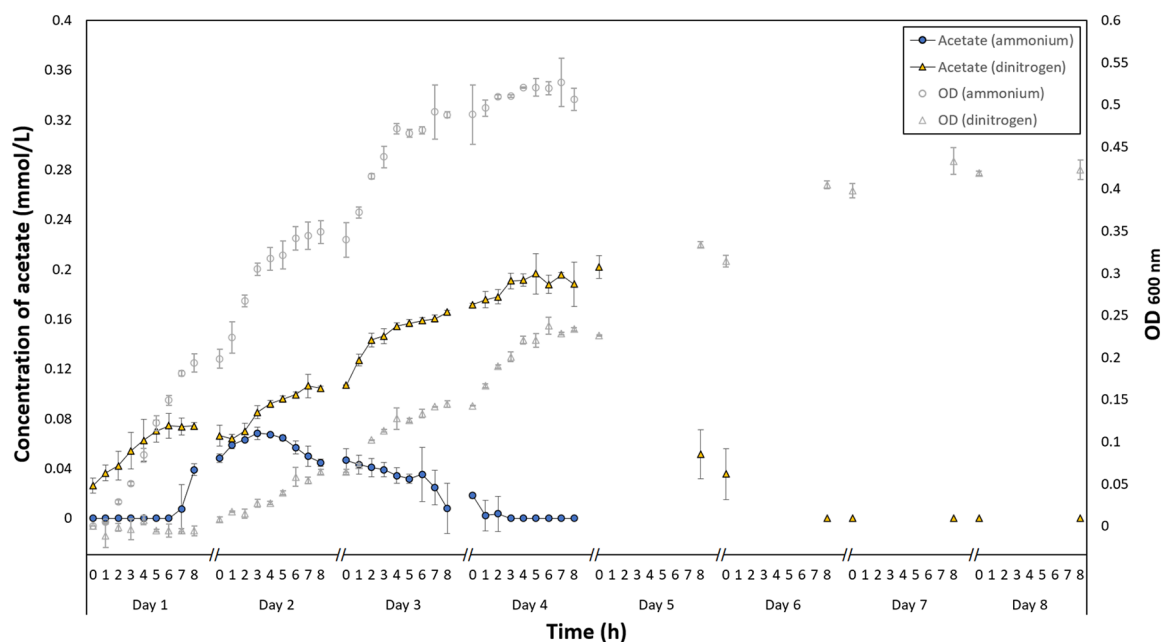


Figure 2. Concentration of acetate (in mmol/L) in ammonium-grown cultures (filled circle, $n=2$) and dinitrogen-grown cultures (filled triangle, $n=2$). The optical density (OD) measured at 600 nm of ammonium (empty circle) and dinitrogen (empty triangle) grown cultures were also shown. The data were collected hourly over an 8-hour period in the first 4 days. For subsequent days, only dinitrogen-grown cultures were monitored, and the data were collected at time $t=0$ and $t=8$ h each day. The symbol // indicates a break in data collection, during which the cultures were kept at 20°C without any shaking. Error bars indicate one standard deviation of the sample data. Some error bars are smaller than the symbols. OD indicates optical density.

also tested with all 3 methods to confirm our detection and measurement of acetate.

Identification of *Acd* in *M. maripaludis* S2 and comparison against other known *Acd*

The genome¹⁸ of *M. maripaludis* S2 was studied using Basic Local Alignment Search Tool (BLAST)¹⁹ with *Acd* in *M. jannaschii* (GenBank accession no. WP_010870094) as a query. MMP0253 was identified as a potential *Acd*. Its primary and secondary structures were compared against the known^{16,20} *Acd* enzymes in *M. jannaschii*, *Haloarcula marismortui* (GenBank accession no. AAV45866) and *Archaeoglobus fulgidus* (GenBank accession no. WP_048095590) using BLAST and HHpred.²¹

Production of recombinant MMP0253

MMP0253 was cloned using the ligation-independent cloning (LIC) technique with pNIC28-Bsa4 as the vector.²² Briefly, the vector was linearised by *Bsa*I and overhangs were created by treating the linear vector with T4 DNA polymerase and deoxyguanosine triphosphate (dGTP). The *acd* insert was amplified by the polymerase chain reaction (PCR) technique with Phusion DNA polymerase and primers. Subsequently, the purified PCR product was treated with T4 DNA polymerase and deoxycytidine triphosphate (dCTP) to create overhangs. The vector and insert were then annealed, and *E. coli* strain Rosetta (DE3) was transformed. The *E. coli* with the recombinant plasmid was cultivated in Terrific Broth (TB) medium at 37°C and 200 rpm. The protein expression was induced by

isopropyl β -D-1-thiogalactopyranoside (IPTG) at 18°C. The recombinant protein was purified by immobilised metal ion affinity chromatography (IMAC) followed by gel filtration.

Test for enzymatic activity

The activity of recombinant MMP0253 was tested at 37°C under oxic conditions. Each assay mixture (0.1 mL) contained 200 mM Tris-HCl (pH 7.7), 5 mM $MgCl_2$, 0.1 mM 5,5'-dithiobis-(2-nitrobenzoic acid) (Ellman's reagent), 0.1 mM Ac-CoA, 0.5 mM ADP, and 5 mM K_2HPO_4 . The absorbance at 412 nm was measured by Infinite 200 PRO (Tecan, Switzerland) before the addition of MMP0253 and 2 min after its addition. Each assay condition was tested in triplicates.

Results

Acetate concentration profiles

All 3 methods (HPLC, GC, and proton NMR spectroscopy) indicated the presence of acetate in our samples. Thus, in spite of its low concentration, there was a high confidence in the acetate detection. Figure 2 shows the acetate concentration profiles in both ammonium and N_2 -grown cultures over multiple days. The 500 MHz proton NMR spectroscopy showed a signal at 1.839 ppm (see Supplementary Material 1), which matches the signal of pure acetate. No acetate was detected in the control sample.

In the ammonium-grown cultures, acetate reached a peak concentration of 0.069 ± 0.005 mmol/L midway through the growth phase on the second day and declined thereafter. In the N_2 -grown cultures, the acetate concentration was non-zero at

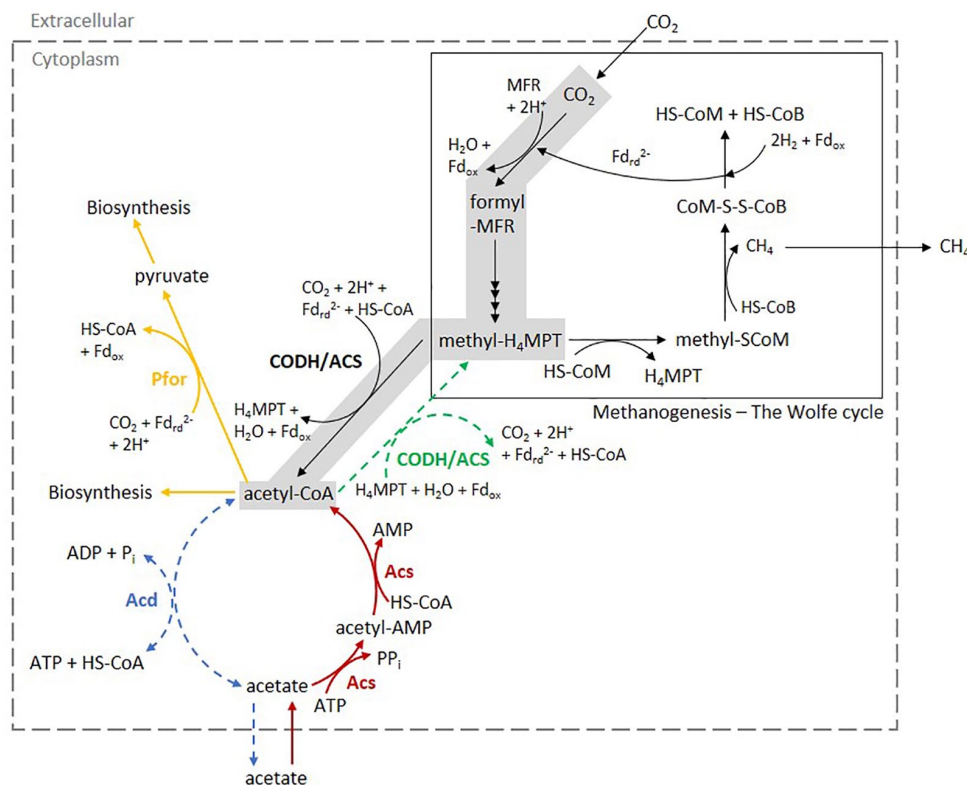


Figure 3. Simplistic view of methanogenesis and biochemical reactions involving acetate and acetyl-CoA. Methanogenesis is shown in the rectangle with solid line border. Grey background indicates the reductive acetyl-CoA pathway. Acetate dissimilation and assimilation were shown. Hypothetical pathways were indicated as dotted lines. Enzymes involved in the Wolfe cycle were not included. Metabolites: acetyl-CoA indicates acetyl coenzyme A; acetyl-AMP, acetyladenylate; ADP, adenosine diphosphate; AMP, adenosine monophosphate; ATP, adenosine triphosphate; Fd_{red}^{2-} , reduced ferredoxin; Fd_{ox} , oxidised ferredoxin; MFR, methanofuran; H_4MPT , tetrahydromethanopterin; HS-CoA, coenzyme A; HS-CoB, coenzyme B; HS-CoM, coenzyme M; P_i , inorganic phosphate; PP_i , inorganic pyrophosphate. Enzymes (bolded): Acd, ADP-forming acetyl-CoA synthetase; Acs, AMP-forming acetate-CoA ligase; CODH/ACS, carbon monoxide dehydrogenase/acetyl-CoA synthase complex; Pfor, pyruvate: ferredoxin oxidoreductase.

the very beginning, which is probably due to the dissimilated acetate in the N_2 -acclimated inoculum. The daily concentration profile exhibited a repeated trend during the first 4 days. It increased at a slowing rate and plateaued near the day's end. The acetate concentration reached a peak of 0.202 ± 0.009 mmol/L on the fourth day, midway through the growth phase. In both ammonium and N_2 -grown cultures, the acetate concentration reached zero as the cells entered the stationary phase.

The overall profiles in both cultures follow an initial rising and subsequent falling trend with a distinct peak characteristic of the acetate switch. In other words, the growth of *M. maripaludis* S2 exhibited 2 phases: an initial acetogenic phase followed by an acetotrophic phase. Acetate assimilation and dissimilation are likely to be competitive and balance each other at the acetate peaks. Both profiles of ammonium and N_2 -grown cultures are markedly similar to the acetate switch profile in *E. coli*.¹ There have been no reports of this for an autotroph in the literature thus far.

MMP0253 showed similarities to other known *Acd*

Our amino acid sequence analysis via BLAST shows that MMP0253 is 35% (e-value: $5.6e-116$) similar to Acd in *H. marismortui*, 44% (e-value: $2.4e-110$) similar to *A. fulgidus*, and

52% (e-value: $9.5e-120$) similar to *M. jannaschii*. These seemingly low percentages do not discredit the claim of MMP0253 as an Acd, because the characterised Acd in *H. marismortui*, *A. fulgidus*, and *M. jannaschii* are also 36% to 42% similar to each other. Our analysis of the 4 secondary protein structures via HHpred showed marked resemblance (see Supplementary Material 2). All 4 have 2 conserved histidine residues (His-242 and His-538 in *M. maripaludis*), which may be analogous to the active sites for the transient phosphorylation in acetate formation.²³ Residues associated with the formation of Ac-CoA binding site and signature motifs of Acd²⁴ can also be found in MMP0253. In essence, the structural evidence at both levels suggests that MMP0253 in *M. maripaludis* is homologous to Acd in the other 3 archaea. Abdel Azim et al,⁸ Goyal et al,²⁵ and Richards et al²⁶ have also annotated MMP0253 as Acd.

MMP0253 catalysed acetate formation from *Ac-CoA*

After recombinant MMP0253 was added into the reagents mixture, a rapid yellow colourisation was observed. Acetate formation from Ac-CoA released coenzyme A (HS-CoA), which reacted with Ellman's reagent to give yellow-coloured

Table 1. Test for the enzymatic activity of MMP0253 at 37°C under oxic conditions.

REAGENTS AND ENZYMES				CHANGE IN ABSORBANCE AT 412 NM
ACETYL-COA	ADP	K ₂ HPO ₄	MMP0253	
X	X	X	X	0.3695 ± 0.0278
	X	X	X	0.1164 ± 0.0081
X		X	X	0.1155 ± 0.0139
X	X		X	0.0772 ± 0.0028
			X	0.0899 ± 0.0255
X	X	X		0.0038 ± 0.0004

Abbreviations: ADP, adenosine diphosphate; X, present in the assay mixture.

Unless indicated otherwise, each assay mixture (0.1 mL) consisted of 200 mM Tris-HCl (pH 7.7), 5 mM MgCl₂, 0.1 mM 5,5'-dithiobis-(2-nitrobenzoic acid) (Ellman's reagent), 0.1 mM acetyl-CoA, 0.5 mM ADP, and 5 mM K₂HPO₄. Absorbance readings at 412 nm were obtained 2 minutes after the addition of MMP0253. For the tests in which MMP0253 was not added, absorbance readings were obtained after 30 minutes. Each assay was done in triplicates.

2-nitro-5-thiobenzoate dianions. Therefore, the observed colourisation (absorbance change of approximately 0.4) confirms the catalytic activity of MMP0253 (Table 1). In the absence of MMP0253, the absorbance change was negligible even after 30 minutes. When Ac-CoA, ADP, or K₂HPO₄ was not added into the reagents mixture, the absorbance change was about 0.1. However, this is due to the interaction between MMP0253 and Ellman's reagent as verified by adding MMP0253 into a mixture of Tris-HCl (pH 7.7), MgCl₂, and Ellman's reagent only. This suggests that the acetate formation from Ac-CoA catalysed by MMP0253 requires all 3 reagents, Ac-CoA, ADP, and inorganic phosphate (P_i).

Discussion

While acetate assimilation by *M. maripaludis* S2 has been reported in the literature,⁷ its dissimilation has not been conclusively established prior to this study. Although one record⁸ of acetate dissimilation does exist for this methanogen, it was limited to the growth with propionate. Our experimental results confirm that *M. maripaludis* S2 can produce acetate when grown in a minimal medium (void of propionate) with either ammonium or N₂ as the nitrogen source. Our preliminary enzymatic study also shows that MMP0253 may function as Acd, which is known¹⁶ to catalyse the reversible formation of acetate from Ac-CoA and generate ATP via substrate-level phosphorylation: Ac-CoA + ADP + Pi ↔ Acetate + ATP + HS-CoA.

Having established acetate dissimilation in *M. maripaludis* S2, we observe that our acetate concentration profiles have a marked resemblance to the acetate switch profile in *E. coli*. Acetate switch, a phenomenon that involves the transition from an acetogenic phase to an acetotrophic phase, has only been observed in heterotrophs (Table 2).¹ Furthermore, all reported microorganisms use the TCA cycle.¹ In contrast, *M. maripaludis* S2 is an autotroph, which uses the Wolfe cycle for methanogenesis (Figure 3).

While we do not have a solid evidence to explain the above acetate profile in this archaeon, we put forth a hypothesis based

on the literature on other microorganisms. It is established¹ that acetate dissimilation in *E. coli* and other heterotrophs serves as a metabolic outlet for carbon overflow, which occurs when their TCA cycles are saturated or inhibited. The dissimilation also helps to reduce Ac-CoA accumulation and recycle HS-CoA. In the late growth phase when the carbon source depletes, these microorganisms assimilate acetate as an additional carbon source. In addition, as acetate accumulates in the growth medium, it diffuses back across the cell membrane. This acidifies the cytoplasm and interferes with other biosynthetic processes.³ The cell removes acetate by converting it into Ac-CoA via a single-step reaction.

Based on the above explanation of the acetate switch in other microorganisms, we can postulate that a similar hypothesis may hold for *M. maripaludis* S2. When the carbon flux into the Wolfe cycle exceeds its capacity, *M. maripaludis* must find a metabolic outlet for the overflow. While the Wolfe cycle has various exits leading to the formations of purines, thymidylate, and methionine, the formation of Ac-CoA from methyl-tetrahydromethanopterin (methyl-H₄MPT) is the largest.³⁷ This may lead to an accumulation of Ac-CoA and diminution of HS-CoA pools, which the cell may avoid via biosynthesis or acetate dissimilation. However, biosynthesis needs ATP, and its primary supply (Wolfe cycle) is already saturated. Hence, acetate dissimilation seems to be the only metabolic outlet to relieve the carbon overflow. While no concrete evidence exists for this hypothesis at the present, we observed that it is consistent with the daily acetate profiles (Figure 2). As our study involved batch culture and CO₂ was replenished daily, the CO₂ supply (flux or overflow) in the liquid medium gradually decreased during each day. As carbon supply decreased over time, carbon overflow decreased, and hence dissimilation decreased and eventually plateaued off. When CO₂ was replenished the following morning, carbon overflow occurred at the start and dissimilation continued at a higher rate than the previous evening.

Table 2. A comparison of the characteristics of the bacteria and archaea with acetate switch.

MICROORGANISM	DOMAIN	TYPE	ACETATE DISSIMILATION ENZYMES	ACETATE ASSIMILATION ENZYMES	REFERENCES
<i>Escherichia coli</i>	Bacteria	Heterotroph	Pta-Ack	Acs Reverse Pta-Ack	Brown et al, ²⁷ Kumari et al ²⁸
<i>Salmonella enterica</i>	Bacteria	Heterotroph	EutD-ACK	Acs Reverse Pta-Ack Reverse EutD-Ack	Starai et al ^{4,29}
<i>Bacillus subtilis</i>	Bacteria	Heterotroph	Pta-Ack	Acs	Grundy et al, ² Presecan-Siedel et al ³⁰
<i>Corynebacterium glutamicum</i>	Bacteria	Heterotroph	No data	Reverse Pta-Ack	Dominguez et al, ³¹ Reinscheid et al, ³² Gerstmeir et al ³³
<i>Vibrio fischeri</i>	Bacteria	Heterotroph	No data	Acs	Studer et al ³⁴
<i>Staphylococcus aureus</i>	Bacteria	Heterotroph	Pta-Ack	Acs	DeMars and Bose ³⁵
<i>Campylobacter jejuni</i>	Bacteria	Heterotroph	Pta-Ack	Acs	Wright et al ³⁶
<i>Mycobacterium tuberculosis</i>	Bacteria	Heterotroph	Pta-Ack	Acs Reverse Pta-Ack	Rucker et al ³
<i>Haloarcula marismortui</i> <i>Haloferax volcanii</i> <i>Halobacterium saccharovororum</i>	Archaea	Heterotroph	Acd	Acs	Brasen and Schonheit ⁵
<i>Methanococcus maripaludis</i>	Archaea	Autotroph	Acd	Acs	This study

Abbreviations: Acd, ADP-forming acetyl-CoA synthetase; Ack, acetate kinase; Acs, AMP-forming acetate-CoA ligase; EutD, *eut* operon-encoded phosphotransacetylase; Pta, phosphotransacetylase.

The hypothesis can also explain the greater acetate dissimilation in N₂-grown cultures. Diazotrophy is an ATP-demanding process.³⁸ Hence, the Wolfe cycle in the N₂ samples will saturate earlier for the same flux of CO₂ (mmol/gDCW/h). Furthermore, the biosynthesis level with N₂ is known³⁹ to be lower. Therefore, the N₂-grown cultures will experience a higher carbon overflow and hence greater acetate dissimilation. Abdel Azim et al⁸ reported an acetate dissimilation when incubating *M. maripaludis* in a minimal medium supplemented with propionate. While they hypothesised that propionate might have reduced the electrochemical proton gradient across the cell membrane, forcing the cell to restore it via the ATP-consuming proton extrusion process, they did not explain why acetate was produced. This ATP-consuming process may have an effect similar to diazotrophy and thus caused acetate dissimilation to occur.

In the late growth phase, *M. maripaludis* transitioned to acetate assimilation. This is possibly due to carbon deficiency, similar to the phenomenon in other microorganisms as discussed earlier. The acidification of the cytoplasm by acetic acid may play a role in inducing *M. maripaludis* to convert it to Ac-CoA; however, further study is needed to verify this.

Acknowledgements

We thank Professors Zhou Zhi (Purdue), Zhou Kang (NUS), Zhao Dan (NUS), Yan Ning (NUS), He Jianzhong (NUS), and Dr Karthika Nagarajan (NUS) for their invaluable help,

guidance, and suggestions during the course of this work. Similarly, we thank Matthew James Rogers (NUS), Prerna Goyal (NUS), Lim Ee Yang (NUS), and Dr Hugo Gerald Schmidt (CARES Ltd). We are indebted to Professor Tong Yen Wah (NUS) and Energy and Environmental Sustainability for Megacities (E2S2) for lending us equipment, which enhanced and expedited our work. We thank Dr Dai Chencheng (CARES Ltd) for his assistance with high-performance liquid chromatography. We thank the NTU Protein Production Platform (www.proteins.sg) for the cloning, expression tests, and purification of protein construct Acd.

Author Contributions

All authors designed the experiment. CHV performed the experiment. All authors wrote and edited the manuscript. All authors read and approved the final manuscript.

Availability of Data and Material

The main datasets generated and/or analysed during the current study are attached as supplementary materials. Any other datasets are available from the corresponding author on reasonable request.

ORCID iDs

Chi Hung Vo  <https://orcid.org/0000-0002-8242-8494>

Markus Kraft  <https://orcid.org/0000-0002-4293-8924>

Supplemental Material

Supplemental material for this article is available online.

REFERENCES

1. Wolfe AJ. The acetate switch. *Microbiol Mol Biol Rev.* 2005;69:12-50.
2. Grundy FJ, Waters DA, Takova TY, Henkin TM. Identification of genes involved in utilization of acetate and acetoin in *Bacillus subtilis*. *Mol Microbiol.* 1993;10:259-271.
3. Rucker N, Billig S, Buckner R, Jahn D, Wittmann C, Bange FC. Acetate dissimilation and assimilation in *Mycobacterium tuberculosis* depend on carbon availability. *J Bacteriol.* 2015;197:3182-3190.
4. Starai VJ, Escalante-Semerena JC. Identification of the protein acetyltransferase (Pat) enzyme that acetylates acetyl-CoA synthetase in *Salmonella enterica*. *J Mol Biol.* 2004;340:1005-1012.
5. Brasen C, Schönheit P. Mechanisms of acetate formation and acetate activation in halophilic archaea. *Arch Microbiol.* 2001;175:360-368.
6. Jones WJ, Paynter MJB, Gupta R. Characterization of *Methanococcus maripaludis* sp. nov., a new methanogen isolated from salt marsh sediment. *Arch Microbiol.* 1983;135:91-97.
7. Shieh JS, Whitman WB. Pathway of acetate assimilation in autotrophic and heterotrophic Methanococci. *J Bacteriol.* 1987;169:5327-5329.
8. Abdel Azim A, Rittmann SKMR, Fino D, Bochmann G. The physiological effect of heavy metals and volatile fatty acids on *Methanococcus maripaludis* S2. *Biotechnol Biofuels.* 2018;11:301.
9. Fricke WF, Seedorf H, Henne A, et al. The genome sequence of *Methanosphaera stadtmanae* reveals why this human intestinal archaeon is restricted to methanol and H₂ for methane formation and ATP synthesis. *J Bacteriol.* 2006;188:642-658.
10. Whitman WB, Ankwarda E, Wolfe RS. Nutrition and carbon metabolism of *Methanococcus voltae*. *J Bacteriol.* 1982;149:852-863.
11. Ekiel I, Smith IC, Sprott GD. Biosynthetic pathways in *Methanospirillum hungatei* as determined by ¹³C nuclear magnetic resonance. *J Bacteriol.* 1983;156:316-326.
12. Westermann P, Ahring BK, Mah RA. Threshold acetate concentrations for acetate catabolism by aceticlastic methanogenic bacteria. *Appl Environ Microbiol.* 1989;55:514-515.
13. Sprott GD, Ekiel I, Patel GB. Metabolic pathways in *Methanococcus jannaschii* and other methanogenic bacteria. *Appl Environ Microbiol.* 1993;59:1092-1098.
14. Rother M, Metcalf WW. Anaerobic growth of *Methanosarcina acetivorans* C2A on carbon monoxide: an unusual way of life for a methanogenic archaeon. *Proc Natl Acad Sci USA.* 2004;101:16929-16934.
15. Hu YJ, Holden JF. Citric acid cycle in the hyperthermophilic archaeon *Pyrobaculum islandicum* grown autotrophically, heterotrophically, and mixotrophically with acetate. *J Bacteriol.* 2006;188:4350-4355.
16. Musfeldt M, Schönheit P. Novel type of ADP-forming acetyl coenzyme A synthetase in hyperthermophilic Archaea: heterologous expression and characterization of isoenzymes from the sulfate reducer *Archaeoglobus fulgidus* and the methanogen *Methanococcus jannaschii*. *J Bacteriol.* 2002;184:636-644.
17. Goyal N, Padhiary M, Karimi IA, Zhou Z. Flux measurements and maintenance energy for carbon dioxide utilization by *Methanococcus maripaludis*. *Microb Cell Fact.* 2015;14:146.
18. Hendrickson EL, Kaul R, Zhou Y, et al. Complete genome sequence of the genetically tractable hydrogenotrophic methanogen *Methanococcus maripaludis*. *J Bacteriol.* 2004;186:6956-6969.
19. Altschul SF, Madden TL, Schaffer AA, et al. Gapped BLAST and PSI-BLAST: a new generation of protein database search programs. *Nucleic Acids Res.* 1997;25:3389-3402.
20. Brasen C, Schönheit P. Unusual ADP-forming acetyl coenzyme A synthetases from the mesophilic halophilic euryarchaeon *Haloarcula marismortui* and from the hyperthermophilic crenarchaeon *Pyrobaculum aerophilum*. *Arch Microbiol.* 2004;182:277-287.
21. Soding J, Biegert A, Lupas AN. The HHpred interactive server for protein homology detection and structure prediction. *Nucleic Acids Res.* 2005;33:W244-W248.
22. Keates T, Cooper CD, Savitsky P, et al. Expressing the human proteome for affinity proteomics: optimising expression of soluble protein domains and in vivo biotinylation. *N Biotechnol.* 2012;29:515-525.
23. Brasen C, Schmidt M, Grotzinger J, Schönheit P. Reaction mechanism and structural model of ADP-forming acetyl-CoA synthetase from the hyperthermophilic archaeon *Pyrococcus furiosus*: evidence for a second active site histidine residue. *J Biol Chem.* 2008;283:15409-15418.
24. Sanchez LB, Galperin MY, Muller M. Acetyl-CoA synthetase from the amitochondriate eukaryote *Giardia lamblia* belongs to the newly recognized superfamily of acyl-CoA synthetases (nucleoside diphosphate-forming). *J Biol Chem.* 2000;275:5794-5803.
25. Goyal N, Zhou Z, Karimi IA. Metabolic processes of *Methanococcus maripaludis* and potential applications. *Microb Cell Fact.* 2016;15:107.
26. Richards MA, Lie TJ, Zhang J, Ragsdale SW, Leigh JA, Price ND. Exploring hydrogenotrophic methanogenesis: a genome scale metabolic reconstruction of *Methanococcus maripaludis*. *J Bacteriol.* 2016;198:3379-3390.
27. Brown TD, Jones-Mortimer MC, Kornberg HL. The enzymic interconversion of acetate and acetyl coenzyme A in *Escherichia coli*. *J Gen Microbiol.* 1977;102:327-336.
28. Kumari S, Beatty CM, Browning DF, et al. Regulation of acetyl coenzyme A synthetase in *Escherichia coli*. *J Bacteriol.* 2000;182:4173-4179.
29. Starai VJ, Garrity J, Escalante-Semerena JC. Acetate excretion during growth of *Salmonella enterica* on ethanolamine requires phosphotransacetylase (EutD) activity, and acetate recapture requires acetyl-CoA synthetase (Acs) and phosphotransacetylase (Pta) activities. *Microbiology.* 2005;151:3793-3801.
30. Presecan-Siedel E, Galinier A, Longin R, et al. Catabolite regulation of the pta gene as part of carbon flow pathways in *Bacillus subtilis*. *J Bacteriol.* 1999;181:6889-6897.
31. Dominguez H, Nezonet C, Lindley ND, Cacaig M. Modified carbon flux during oxygen limited growth of *Corynebacterium glutamicum* and the consequences for amino acid overproduction. *Biotechnol Lett.* 1993;15:449-454.
32. Reinscheid DJ, Schnicke S, Rittmann D, Zahnow U, Sahn H, Eikmanns BJ. Cloning, sequence analysis, expression and inactivation of the *Corynebacterium glutamicum* pta-ack operon encoding phosphotransacetylase and acetate kinase. *Microbiology.* 1999;145:503-513.
33. Gerstmeir R, Wendisch VF, Schnicke S, et al. Acetate metabolism and its regulation in *Corynebacterium glutamicum*. *J Biotechnol.* 2003;104:99-122.
34. Studer SV, Mandel MJ, Ruby EG. AinS quorum sensing regulates the *Vibrio fischeri* acetate switch. *J Bacteriol.* 2008;190:5915-5923.
35. DeMars Z, Bose JL. Redirection of metabolism in response to fatty acid kinase in *Staphylococcus aureus*. *J Bacteriol.* 2018;200:e00345-18.
36. Wright JA, Grant AJ, Hurd D, et al. Metabolite and transcriptome analysis of *Campylobacter jejuni* in vitro growth reveals a stationary-phase physiological switch. *Microbiology.* 2009;155:80-94.
37. Thauer RK. The Wolfe cycle comes full circle. *Proc Natl Acad Sci USA.* 2012;109:15084-15085.
38. Hoffman BM, Lukoyanov D, Yang ZY, Dean DR, Seefeldt LC. Mechanism of nitrogen fixation by nitrogenase: the next stage. *Chem Rev.* 2014;114:4041-4062.
39. Kessler PS, Daniel C, Leigh JA. Ammonia switch-off of nitrogen fixation in the methanogenic archaeon *Methanococcus maripaludis*: mechanistic features and requirement for the novel GlnB homologues, NifI(1) and NifI(2). *J Bacteriol.* 2001;183:882-889.